Hindawi Publishing Corporation
Advances in Materials Science and Engineering
Volume 2016, Article ID 5810216, 10 pages
http://dx.doi.org/10.1155/2016/5810216

Research Article

Fabrication of Electrospun Chitosan/Nylon 6 Nanofibrous Membrane toward Metal Ions Removal and Antibacterial Effect

Akram R. Jabur, Laith K. Abbas, and Saja A. Moosa

Department of Materials Engineering, University of Technology, Baghdad, Iraq

Correspondence should be addressed to Akram R. Jabur; akram.jabut@gmail.com

Received 31 July 2016; Revised 14 September 2016; Accepted 11 October 2016

Academic Editor: Luiz F. de Moura

Nylon 6/Chitosan membranes were fabricated by electrospinning onto a Millipore glass fiber filter to produce nanofibrous filter. Scanning electron microscopy (SEM) and water contact angle (WCA) were done to characterize the produced filter. Filter removal capability (adsorption) for metal ions was investigated for lead nitrate ($Pb(NO_3)_2$) and sodium chloride (NaCl). The antibacterial effect of the Nylon 6/Chitosan was investigated for *Escherichia coli*. Removal optimum values for $Pb(NO_3)_2$ and NaCl reached 87% and 75%, respectively. This research demonstrated that Nylon 6/Chitosan nanofibrous membrane has an enormous applicable potential removal for metal ions from aqueous solutions, antibacterial activity reaching 96%, and reasonable inhibition zone against *Escherichia coli* (*E. coli*).

1. Introduction

Removal of pathogens, chemicals, and heavy metals to produce clean drinking water is the most important factor that water purification focuses on. Polymer gels and several polymer solutions were electrospun to produce filters that were able to remove these contaminates. Most common used electrospun polymers are chitin [1], Chitosan derivative [2], Poly(ethylene-vinyl alcohol) [3], Poly(glycolic acid) and chitin [4], and Chitosan/PVA [5]. Recently, Chitosan and its derivatives had gained a lot of interest because of the wide range of applications in biomedicine, bioseparation, and food science. Chitosan, which is deacetylate's product of chitin (produced from the crust of crustacean shells), has desirable properties such as biofriendly, biodegradable, and antibacterial compound [6]. Also, Chitosan and chitin are able to remove metals and dyes so that they can be used to clean water; this is due to the adsorption of the metals and dyes to the cationic amine functional groups on chitosan. Various cross-linked polysaccharide materials with Chitosan can remove different metal and dye pollutants [7]. Chitosan and chitin also had the ability to remove polycyclic aromatic hydrocarbons more effectively [8]. Removal of particles like As^{+5} (arsenic) can be effected by the degree of deacetylation (DD). Adsorption and removal of particles in water can be influenced by crystallinity. Crystallinity increased by the amine group which forms a hydrogen bond to other chitosan monomers, and this affects the fiber morphology and adsorption [9]. Negatively charged dye like reactive Black 5 can be removed by Chitosan. It can positively charge in an acid environment and electrostatic forces are responsible for dye removal. It had been mentioned in the results that changing the molecular weight (MW) of chitosan from 80,100 to 308,300 reduces chitosan's ability to adsorb dye [10, 11]. This is because the changing in the internal structure of the chitosan chains and hydrogen bonding between hydroxyl and amine groups which reduced the possibility of dye binding. It had been found that the number of amine groups, determined by the DD, was affected by the removal of metal ions in water. High DD value (97%) produced higher removal efficiency, comparing to chitosan with 52% of DD value [11, 12]. Finally, nanofibers and in particular Chitosan nanofibers are better in removing metals, chemicals, and bacteria from water [11].

2. Experimental Part

2.1. Materials. The materials used in this research are Nylon 6 and formic acid, which were purchased from Sigma-Aldrich Co. (USA), molecular weight for repeat unit was 113.16 g/mol, and the total molecular weight was 25,000 g/mol. Chitosan

was purchased from Cheng Du Micxy Chemical Co. Ltd. with the degree of deacetylation ((DD) ≥ 90%), molecular weight for repeat unit was 161.16 g/mol, and the total molecular weight was Mw 338,000. Lead nitrate ($Pb(NO_3)_2$) was purchased from Fluka Chemika, Germany (molecular weight 331.2 g/mol), sodium chloride (NaCl) was purchased from Edutek Chemicals, India (molecular weight 58.44 g/mol), and all agents were used without further purification. Micropore glass filter with binder (technical microfilter) has pore size of 2 μm, porosity of 90%, thickness of 1.2 mm, and fiber diameter of 124 mm.

2.2. Preparation of Nylon 6/Chitosan Blend Electrospinning Solution. Nylon 6 pellets and Chitosan powder at a concentration of 25% wt were blended in formic acid solution (25% wt/v) at 30°C using a laboratory magnetic stirrer for three hours to ensure complete dissolution of solutes and obtain a homogenous solution. Various ratios of Nylon 6/Chitosan (100/0, 90/10, 80/20, and 70/30) were utilized to prepare the blended nanofibrous membranes.

2.3. Electrospinning. The prepared electrospun solution was collected in 10 mL syringe equipped with a 22-gauge stainless steel needle tip. The electrospinning process was carried at 25 kV voltage, 0.5 mL/hr flow rate, 0.7 mm needle diameter tip, and 15 cm distance between electrodes. The electrospinning process took four hours' time and these parameters will be fixed for all the following solutions. The electrospinning process was carried out at room temperature of 25 ± 1°C and relative humidity of 25–30%. The prepared electrospun nanofiber sheet has an area of 153.86 cm^2 and diameter of 14 cm, whereas the weight of the prepared electrospun nanofiber sheet equals 0.0035 g for 1 cm^2. The electrospinning process was carried out by a bioelectrospinning/electrospray system (ESB-200), provided by (Nano NC, South Korea), which is shown in Figure 1.

2.4. Characterization. Scanning electron microscopy (Model: VEGA3 LM-TESCAN) was used in studying the surface morphology of nanofibers. Low variable pressure was used in all SEM tests for all specimens, the pressure was enough, and there was no need for any more of sample gold ion sputtering coating to chive conductivity on the surface of the specimens in SEM tests. Specimen conductivity was measured by a model (C and 7110 Inolab). Solution viscosity was measured by a viscometer of type DV-II-pro at room temperature (25 ± 1°C). Solution surface tension was measured by surface tensiometer model (JYW-200A-Laryee Technology Co.) using a ring of platinum. Solution electrical conductivity was measured using the electrical conductivity device of model (C and 7110 Inolab).

2.5. Contact Angle Measurement. The wettability of the electrospun mats was measured with deionized water contact angle measurements. Contact angle meter of the type CAM 110, Germany, was used. Deionized water was automatically dropped onto the membrane. Measurement was carried out in three seconds.

2.6. Permeability Test. Experiments were carried out at a temperature of 25 ± 1°C. Tests were done and conducted by using pressure cross flow filtration system. The diameter of membrane filter sample was 30 mm. Measuring pure water flux and salt rejection was the used method that characterized Nylon 6 with various additives membranes. Membranes were exposed to a pressure with the value of 1 bar for 50 min. They were placed with a shim and a mesh structured spacer to eliminate pressure polarization. They were pressurized with a mechanical pump controlled by pressure regulators and then the pressure was controlled to the operating pressure (1–6 bar). Figure 2 shows pressure cross flow filtration system which is designed especially to conduct the test. The permeable flux was calculated by

$$J = \frac{V}{A \times T}, \tag{1}$$

where J is the permeable flux (L/m^2× h), V is the volume of permeate (liter), A is the effective membrane surface area (m^2), and T is the time (hour).

The salt rejection was determined using atomic absorption device (AA-7000 atomic absorption spectrophotometer, Shimadzu). The rejection of salts was obtained by

$$R = \left(1 - \frac{C_p}{C_f}\right) \times 100\%, \tag{2}$$

where C_p and C_f are ion concentration in permeate and feed, respectively, and (R) is rejection as a percentage. Figure 2 shows the system used in this process. During the rejection test three cells of membranes (three layers) on one layer of microfiber were used to increase the relation ratio.

2.7. Mechanical Strength Measurement. Mechanical properties of the electrospun membrane were measured by a tensile mechanical tester of the type Tinus Olsen, H50 KT. A (5 N) load cell was used in that device. Specimen thicknesses were measured by an optical microscope. Specimens with 10 mm dimensions width and 100 mm length were tested and the extension rate at the room temperature was 0.5 mm/min. The experiments were carried out three times to calculate the average value of the results.

2.8. Antimicrobial Test

2.8.1. Antibacterial Activity Test (Disc Diffusion Method). Bacteria were grown aerobically in nutrient broth at 37°C for 12 hours [13]. Cells were washed and suspended in distilled water until reaching the final concentration of 10^6 CFU/mL. The antimicrobial susceptibility of Nylon 6 nanofibers/Chitosan was evaluated using the disc diffusion method. "Muller-Hinton agar" was prepared from a commercially available dehydrated medium according to manufacturer's instructions. The dried surface of "Muller-Hinton agar" plate was inoculated with *E. coli* by swabbing over entire the sterile agar surface. Two forms of nanofiber sterilized membrane samples were cut into small standard circles (6 mm in diameter) for each circle and placed on the surface of the inoculated media.

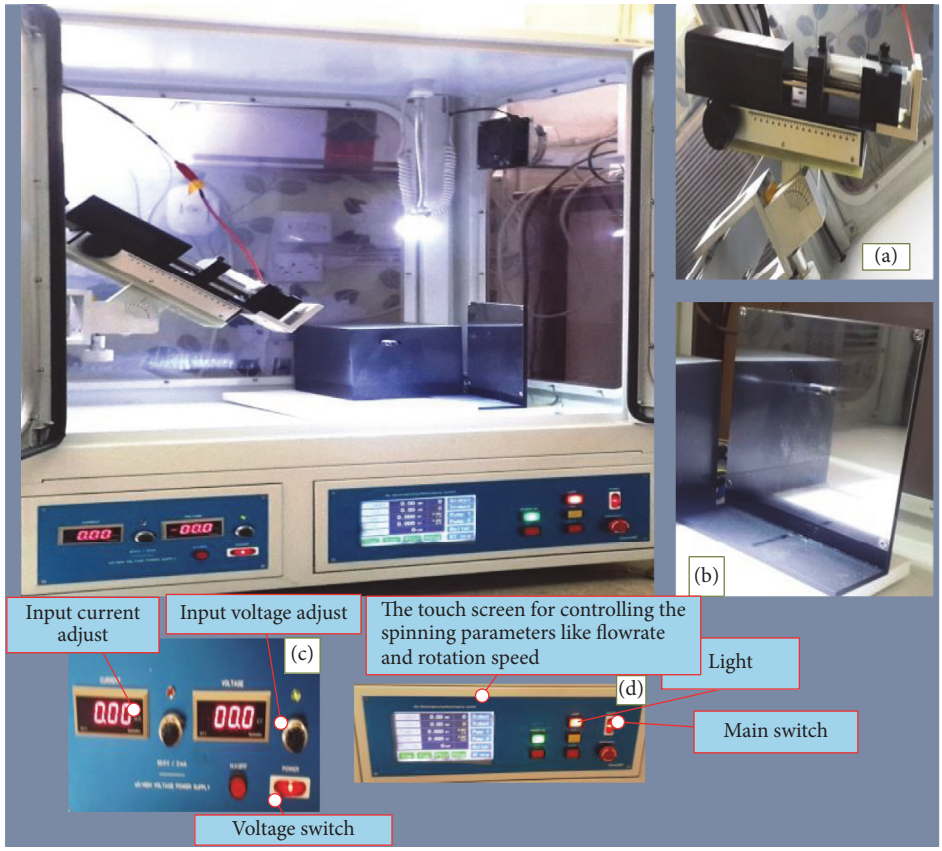

Figure 1: Electrospinning device: (a) syringe pump instruction, (b) collector plate, (c) power supply, and (d) touch control board.

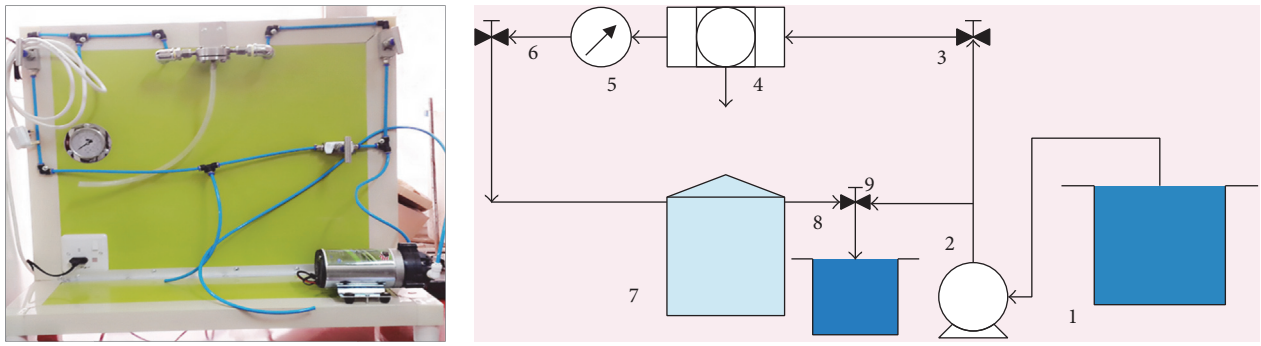

(a) (b)

Figure 2: (a) Pressure cross flow image of filtration system. (b) Schematic diagram of the filtration system process. 1: tank for water sample test. 2: pump. 3: entry valve. 4: filter/module. 5: pressure gauge. 6: outlet valve. 7: open tank for permeate water sample. 8: tank of rejected water sample. 9: recycle valve.

The first form of nanofiber membrane contains additive and the other one without additive was used as a control. The plates were incubated at 37°C for 24 hours. Incubation plates then were examined in order to identify zones of on growth characteristic for antibacterial activity (halos around the fragments).

2.8.2. Antibacterial Activity Test (Optical Density Method). The antibacterial activity of electrospun nanofibers membrane was also tested by immobilizing nanofiber onto filters of a Millipore under vacuum filtration. A test water sample was prepared by inoculating 1×10^8 cells/mL *E. coli* into 250 mL of sterile normal saline water sample (0.85% NaCl in 100 mL distilled water). Water samples then were filtered through the membrane. After this step the optical density of the solution was measured by UV spectrophotometer (UV-1800 spectrophotometer, Shimadzu) at 450 nm wavelength. The number of bacteria was indirectly measured by optical density in an ultraviolet (UV) visible spectrometer and the

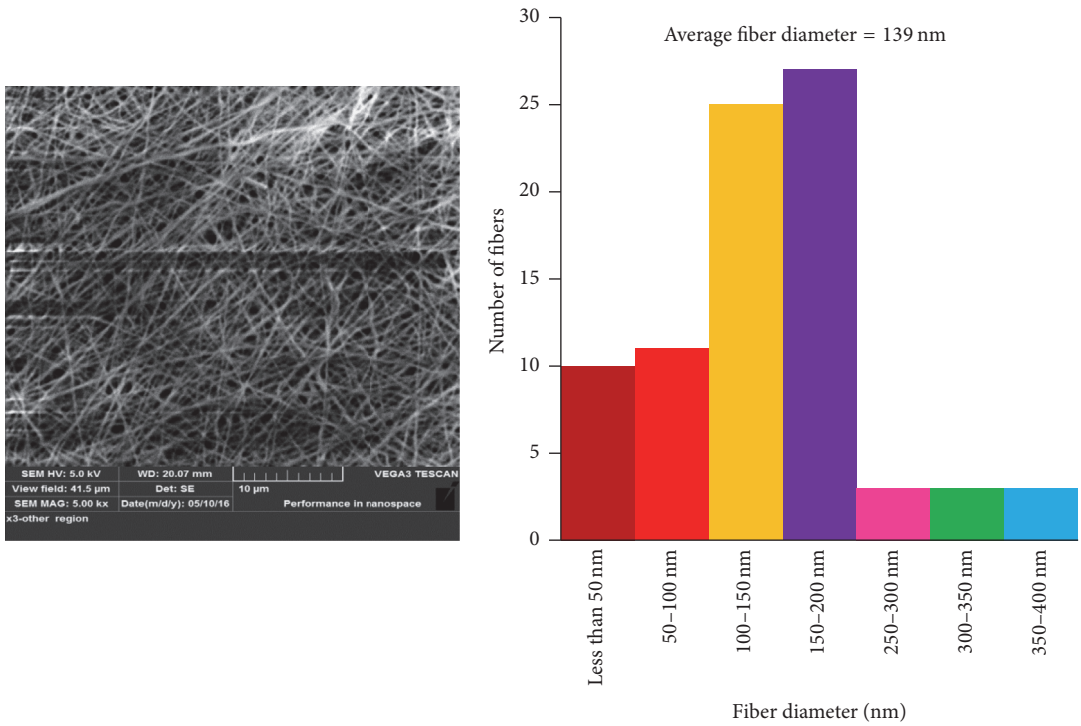

Figure 3: (a) SEM image of pure Nylon 6 nanofibers membrane and (b) fiber diameter distribution.

antibacterial activity was evaluated quantitatively with the following equation:

$$\text{Antibacterial activity (Efficiency)} = \frac{A - B}{A} \times 100\%, \quad (3)$$

where A and B are the numbers of surviving cells in the control and test samples, respectively [14].

3. Results and Discussion

3.1. Properties of Spinning Solutions. Viscosities of Nylon 6 and Nylon 6/Chitosan solutions at various concentrations were shown in Table 1. Adding Chitosan in Nylon 6 solution led to increase the viscosity with increasing Chitosan content. Chitosan molecules seem to be very large when compared with Nylon molecules [15].

Table 1 shows the effect of Chitosan on electrical conductivity which had increased because of the increase of the Chitosan; this result agreed with "Bizarria et al.," whose result shows improving in electrical conductivity with increase in Chitosan concentration when using Chitosan blended with PEO [16]. It is obvious that the surface tension increased with increasing Chitosan concentration due to high solution viscosity, but there is no significant change in surface tension.

3.2. Electrospun Membrane Characterization. Nanofibers (SEM) images of nanofiber diameter histogram distribution are shown in Figure 3. Figure 3(a) represents the Nylon 6/Chitosan (100/0) nanofibers with an average diameter of 139 nm and the desirable morphology had been obtained. The nanofiber diameter increased with the increasing of Chitosan content in the blended solution and this is because of the increasing in the viscosity of the solution. Figure 4(a) shows an increase in fiber diameter and this had been happing because of very high viscosity values and there is difficulty in the ejection of jets from polymer solution and it results in a larger fiber diameter. This result had been matched with "Deitzel et al." [17]. The desirable morphology had been converted to a defective structure with the increasing of the Chitosan content in the blend solution. Experiments showed that increasing of Chitosan ratio above 30% will rise the solution viscosity in which electrospinning became impossible. Usually fouling decreases with an increase in hydrophilicity of the polymeric material. In fact, a decrease in contact angle leads to increase in the flux ratio, which means decreased fouling [18]; therefore, evaluating the membrane characteristics was followed by contact angle measurements. Figure 5 shows the contact angle values of droplet with nanofibrous membranes after 3-second contact.

Water contact angle (WAC) for pure Nylon 6 nanofiber reaches the value 70 while the WAC of Nylon 6/Chitosan at a weight ratio of 70/30 reaches the value of 12.8. The results indicate a significant improvement in hydrophilicity of a membrane which is increased by increasing the Chitosan content. This can be attributed to the presence of a large number of functional groups like acetamide, primary amino, and/or hydroxyl groups in Chitosan structure. These outcomes agreed with the work reported by "Zhang et al." [19].

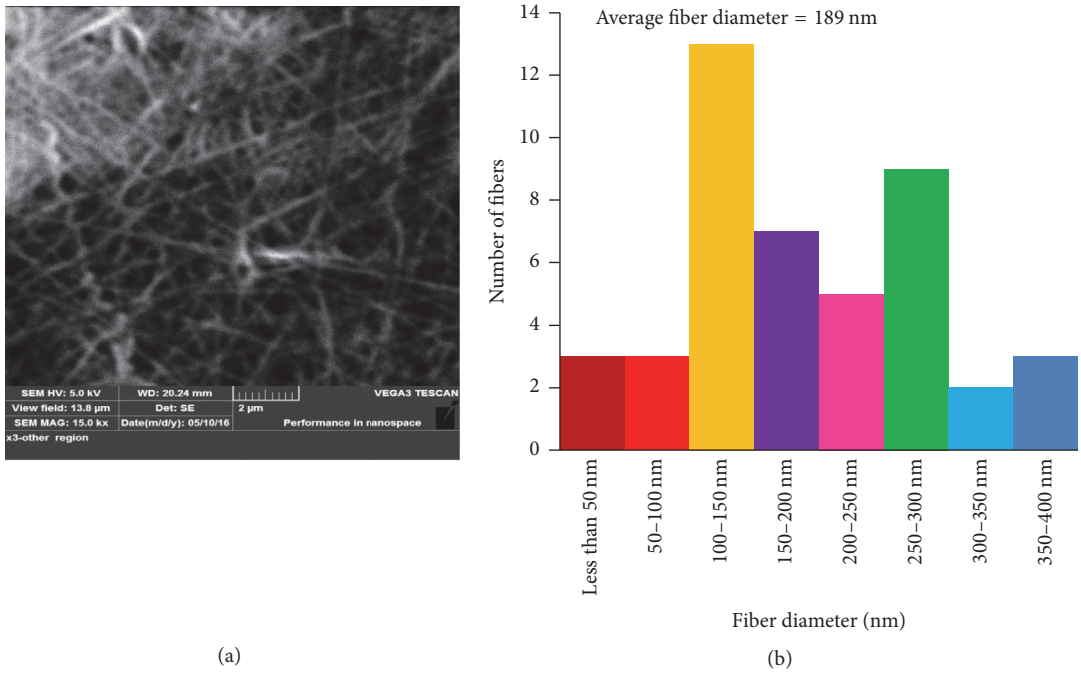

Figure 4: (a) SEM image of (30/70) Chitosan/Nylon 6 nanofibers membrane and (b) fiber diameter distribution.

Table 1: The electrospinning solution properties (these average values after three-time test).

Chitosan/Nylon ratio	Electrical conductivity (σ: mS/cm)	Viscosity cP	Surface tension (mN/m)
0/100	4.00	692	34.430
10/90	6.02	6467	36.610
20/80	7.40	11350	38.532
30/70	8.33	17300	39.452

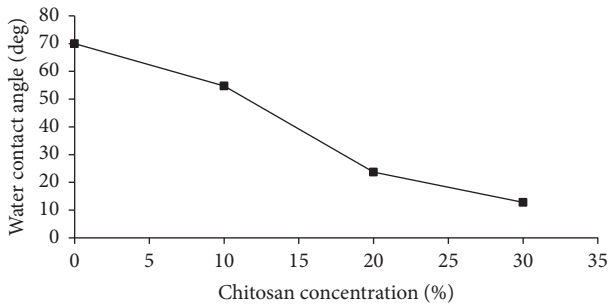

Figure 5: Water contact angle variations of various Nylon/Chitosan electrospun nanofibrous membranes.

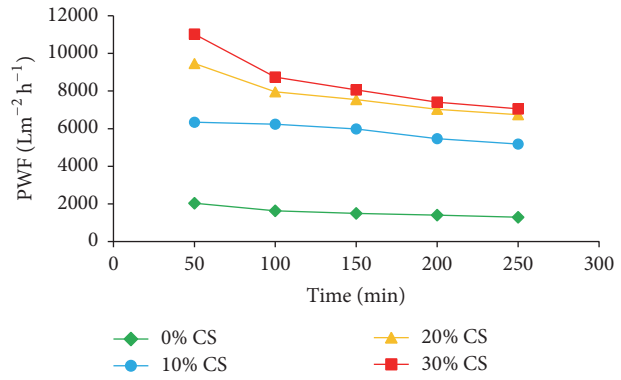

Figure 6: Pure water permeation flux with time of Nylon 6/Chitosan nanofiber membrane at room temperature and 1-bar pressure.

Figure 6 shows the behavior of pure water permeation flux with time at room temperature and 1-bar membrane pressure. It was found that the pure water permeation flux of Nylon 6/Chitosan nanofiber fiber membrane decreases with time from 2037.063 to 1293.53 (l/m^2·hr) for 0/100 Nylon 6/Chitosan. Figure 6 shows that flux has been improved as the concentration of Chitosan increased because Chitosan increases the hydrophilicity of the membrane, whereas the relationship between flux and pressure is explained in Figure 7 which represents that when the pressure increased the flux permeates increased, because flux is directly proportional to the pressure drop across the membrane as shown in Figure 7, the same behavior for all membranes as the pressure increased.

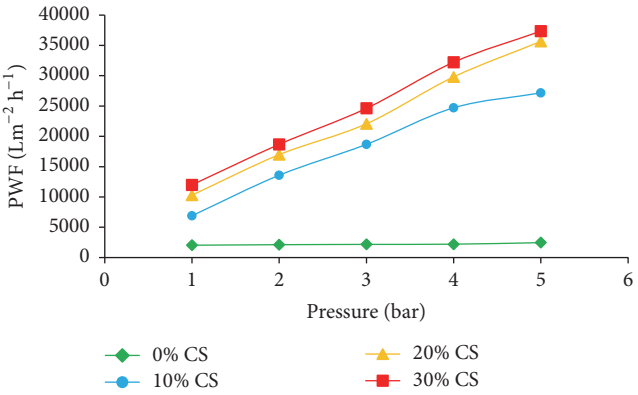

Figure 7: Effect of membrane pressure on the pure water permeation flux of the Nylon 6/Chitosan nanofiber membrane.

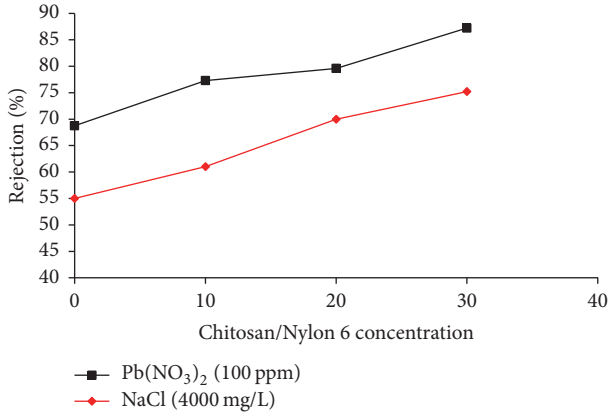

Figure 8: Effect of Nylon 6/Chitosan ratio on rejection of $Pb(NO_3)_2$ salt and NaCl Salt aqueous solutions with initial concentration 100 ppm and 4000 mg/L, respectively, at room temperature and 1 bar.

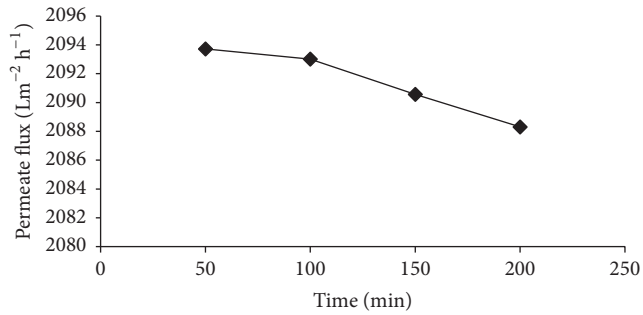

Figure 9: Effect of time on flux of water containing 100 ppm $(Pb(NO_3)_2)$ for Nylon/10% Chitosan membrane at room temperature and 1 bar.

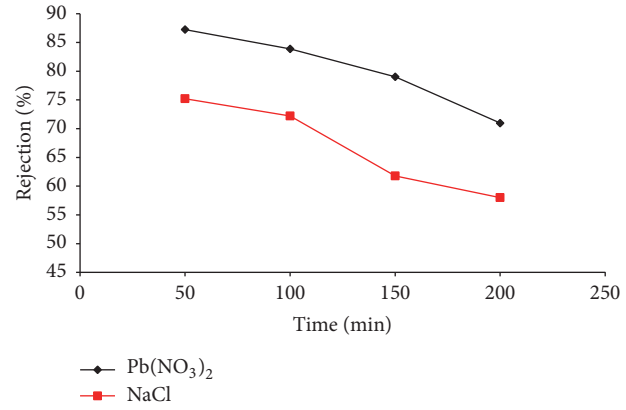

Figure 10: Effect of time on rejection (%) of $Pb(NO_3)_2$ and NaCl for Nylon/30% Chitosan membrane at room temperature and 1 bar.

The transport mechanism within membrane can be explained on the basis of the solution diffusion model. According to this model, transport process within the membrane involves three steps: (1) sorption at the surface of the membrane, (2) diffusion into the membrane, and (3) desorption. The hydrophilic nature of Chitosan acts as driving force for sorption of water into membrane [20].

The presence of an amine and hydroxyl groups on Chitosan developed hydrogen bonding and Van der Wall's forces which caused a change in hydrophilicity of blended membranes [20]. Due to increase electrostatic interactions, extensive cross-linkage was developed which helped in the exclusion of salt ions [20]. Chitosan and chitin had been shown to remove metals and dyes so that they can be used to clean water [7]. Various cross-linked polysaccharide materials with Chitosan can remove different metal and dye pollutants [7]. Figure 8 shows the effect of Chitosan on the rejection percentage for $Pb(NO_3)_2$ and NaCl. When the Chitosan concentration had been increased, rejection increases functional groups and electrostatic interaction. In general, increasing Chitosan concentration will increase the expulsion of metal ions due to increase in functional groups and the electrostatic force which kept within electrospun nanofiber during the electrospinning process. Another important factor of electrospun nanofiber membrane high surface area provides excessive adsorption sites for metal ions and dye adsorption and the higher porosity leads to smaller driving forces to push the water through the membrane which makes the process less energy intensive and facile [21]. Chitosan has high contents of amino and hydroxyl functional groups. Owing to these properties, Chitosan is widely used in removal of contamination from wastewater [21].

Among the salts potassium sulphate showed more flux and rejection followed by sodium chloride. This can make it clear with the assistance of ionic size and charge density. The high rejection of K^+ ion reaches the value of 80% for the membrane (PEI) and this is because of the higher ionic radius of K^+ ion, where its value is 157 pm compared with the value of 116 pm for Na^+ [22]. This clarified why the high rejection ratio of Pb^{+2} ion and rejection ratio proportion came up to 87% and Na^{+1} ion up to 75%. Nanofiber adsorption methods show that nanofibers are the best to remove metal ions while having low pressure drops and high water fluxes. Figure 9 shows the effect of time on the flux which decreases as the time increases due to membrane fouling. Figure 10 shows the efficiency of salt ions removal which also decreases with time which indicates the effect of Chitosan decrease with time.

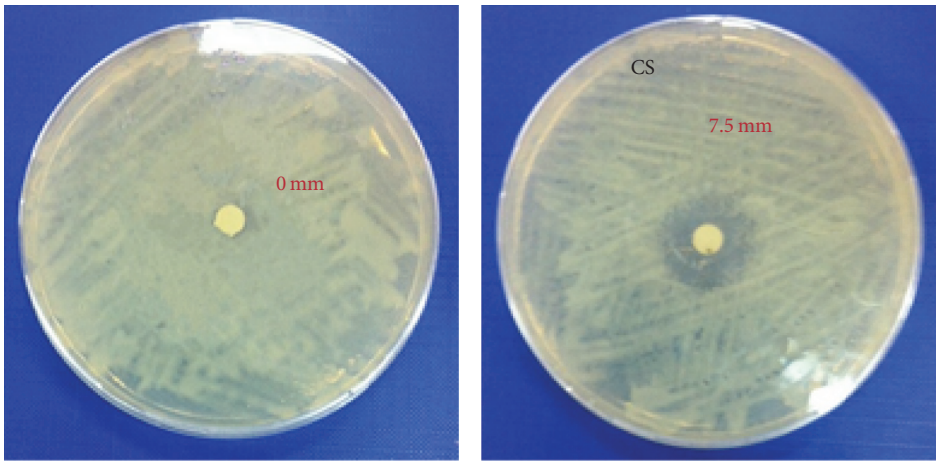

Figure 11: The formation inhibition zone around the Chitosan/Nylon 6 membrane after 24 hours and 37°C.

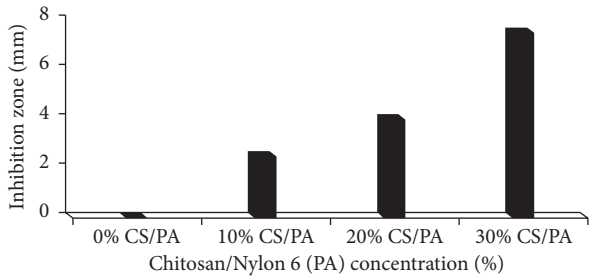

Figure 12: Effect of Chitosan/Nylon 6 ratio on inhibition zone against *E. coli*. bacteria.

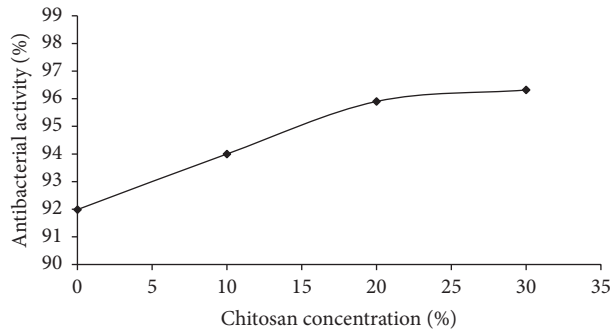

Figure 13: Effect of Chitosan addition on the antibacterial activity.

3.3. Antibacterial Activity Results. The Chitosan is known for its antimicrobial activity. Generally, it is accepted to say that the amine group of Chitosan can react with the anionic groups on the bacterial cell surface. Such interaction brings extensive change to the cell surface and the cell permeability [23–25]. Leakages of intracellular substances can be caused by cell permeability leading to cell death. This mechanism has been demonstrated by electron microscopy [26]. When amine groups increase the charge of the Chitosan will increase and that will cause a stronger interaction between Chitosan and cells. Figure 12 shows the effect of Chitosan on *E. coli* bacteria and the measure in the inhibition zone of 30/70-Chitosan/Nylon 6 which reached up to 8 mm and increasing the Chitosan percentage increases the inhibition zone. Figure 11 shows the formation of inhibition zone around the Chitosan/Nylon membrane.

Figure 13 shows the antibacterial activity and when the Chitosan concentration increases the antibacterial activity increases to 96% at 30/70-Chitosan/Nylon ratio. SEM image shows how the electrospun nanofiber captures and prevents the bacteria from penetrating into water, as in Figure 14.

3.4. Mechanical Test Result. The tensile strength of prepared membranes was given in Figures 15 and 16. In this research the mean tensile strength of Nylon membranes was 1.45 MPa. The tensile strength of 10/90-Chitosan/Nylon 6 membrane (2.844 MPa) was slightly higher than that of pure Nylon membrane, the tensile strength of 20/80-Chitosan/Nylon 6 membrane was 4.1 MPa, and 30/70-Chitosan/Nylon 6 membrane was 4.5 MPa. Clearly, Chitosan/Nylon 6 membrane had the highest tensile strength. There is an increase in the tensile strength of Chitosan/Nylon 6 electrospun membrane with the increase in Chitosan percentage.

3.5. Results Statistical Analysis. The standard deviation was calculated from the results obtained in Figures 5, 8, 10, and 11, which can be seen in Table 2.

As can be seen, the results of standard deviation calculations showed that increasing the wt.% of Chitosan led to making water contact angle the most affected result, which made it the most significant result, while the antibacterial activity (%) was the lowest significant result. Standard deviation calculation of rejection (%) for NaCl salts and $Pb(NO_3)_2$ salts gives a different indication as is seen, it gives an opposite indication for rejection (%) for NaCl salts, and this cannot be considered as a final result and the results obtained in Figure 8 are more reasonable because of the difficulty of capturing the ions of NaCl salts comparing with the ions of $Pb(NO_3)_2$ salts. Table 3 illustrates the standard deviation calculation for a

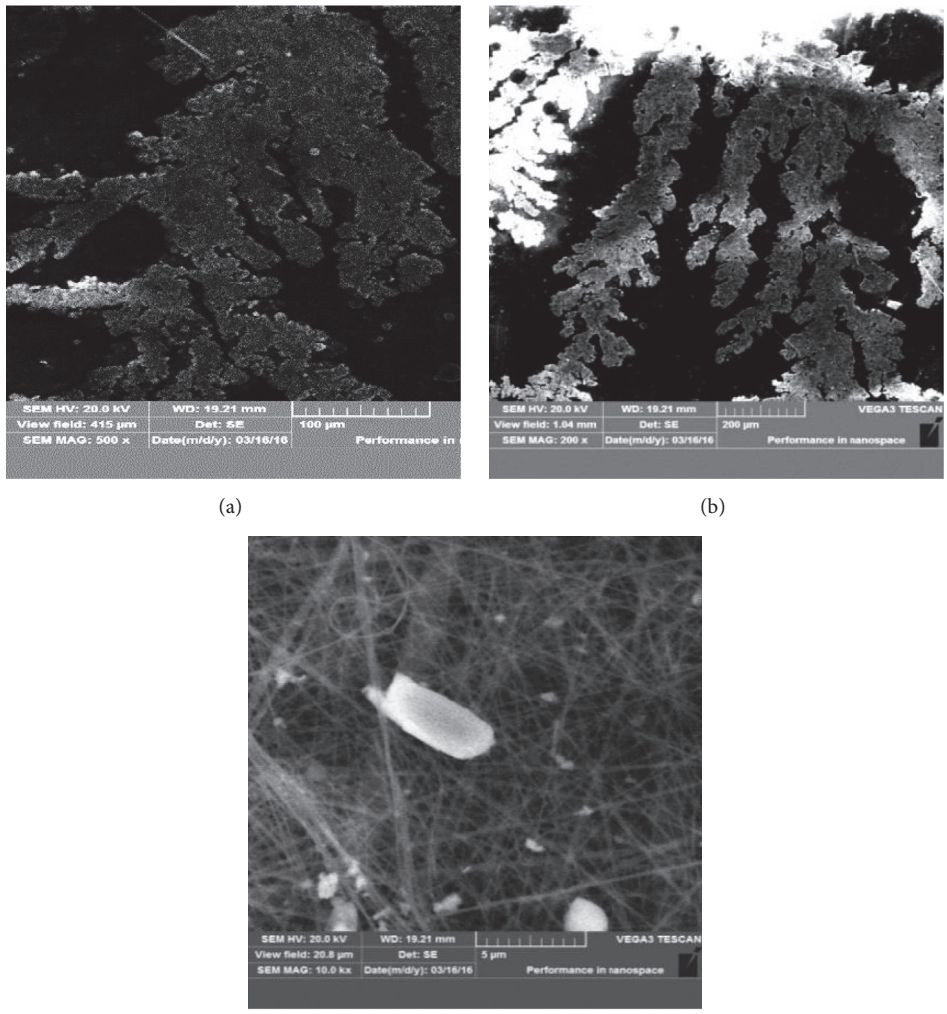

Figure 14: SEM of membrane after being exposed to bacteria, where (a) and (b) show the bacteria cluster on the membrane surface as a dendritic shape colony and (c) shows how fiber captures the bacteria.

Table 2: Standard deviation calculation of water contact angle, rejection %, inhibition zone against *E. coli.* bacteria, and antibacterial activity (%) results.

Results	Water contact angle (deg.)	Rejection % of NaCl salts (4000 mg/L)	Rejection % of $Pb(NO_3)_2$ salts (100 ppm)	Inhibition zone against *E. coli* bacteria (mm)	Antibacterial activity (%)
Standard deviation value	26.60	9.03	7.61	3.13	1.98

strain of the nanofiber membrane and its strength with the increase of the wt.% of Chitosan.

As it can be seen, the increase of the wt.% of Chitosan to 30% increases the strain of the membrane and also increases its tensile strength which is a desirable efficient factor.

4. Conclusions

Chitosan/Nylon 6 nanofiber membranes were prepared via electrospinning by mixing different amounts of Chitosan with Nylon 6. The addition of Chitosan improves the hydrophilicity and mechanical strength of Nylon 6 nanofiber membrane. The enhanced hydrophilicity of the nanofiber membrane can decrease the antifouling effect to make the mat a potential candidate for water filtration and improve the performance of membrane at low pressures. The Chitosan blended with Nylon 6 membranes showed better bactericidal ability as compared to the neat Nylon 6 membranes. Water filter media with a high rejection ratio against heavy metals ions reached 87% at 30/70-Chitosan/Nylon membrane.

Table 3: Standard deviation calculation for tensile strength and strain of the nanofiber membrane.

Results	Membrane strain (%)				Membrane tensile strength (MPa)
	0% CS	10% CS	20% CS	30% CS	
Standard deviation value	0.44	0.84	1.26	1.50	1.37

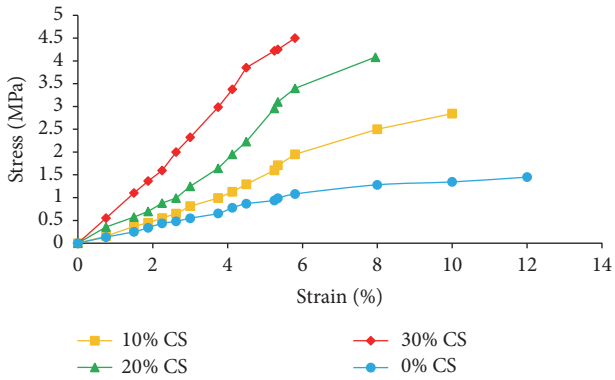

Figure 15: Stress-strain curve of Chitosan/Nylon 6 with various ratios.

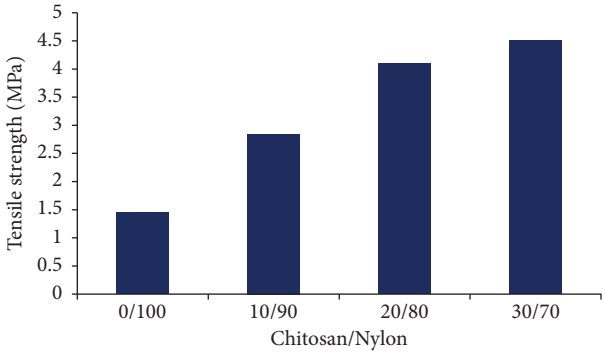

Figure 16: Chitosan/Nylon 6 ratio effect in mechanical strength.

Competing Interests

The authors declare that there is no conflict of interests regarding the publication of this paper.

References

[1] M. C. McManus, E. D. Boland, D. G. Simpson, C. P. Barnes, and G. L. Bowlin, "Electrospun fibrinogen: feasibility as a tissue engineering scaffold in a rat cell culture model," *Journal of Biomedical Materials Research Part A*, vol. 81, no. 2, pp. 299–309, 2007.

[2] S. M. Alipour, M. Nouri, J. Mokhtari, and S. H. Bahrami, "Electrospinning of poly(vinyl alcohol)-water-soluble quaternized chitosan derivative blend," *Carbohydrate Research*, vol. 344, no. 18, pp. 2496–2501, 2009.

[3] S. Chuangchote and P. Supaphol, "Fabrication of aligned poly (vinyl alcohol) nanofibers by electrospinning," *Nanoscience and Nanotechnology*, vol. 1, pp. 125–129, 2006.

[4] W. H. Park, L. Jeong, D. I. Yoo, and S. Hudson, "Effect of chitosan on morphology and conformation of electrospun silk fibroin nanofibers," *Polymer*, vol. 45, no. 21, pp. 7151–7157, 2004.

[5] Y. Zhang, X. Huang, B. Duan, L. Wu, S. Li, and X. Yuan, "Preparation of electrospun chitosan/poly(vinyl alcohol) membranes," *Colloid and Polymer Science*, vol. 285, no. 8, pp. 855–863, 2007.

[6] I. Aranaz, M. Mengíbar, R. Harris et al., "Functional characterization of chitin and chitosan," *Current Chemical Biology*, vol. 3, no. 2, pp. 203–230, 2009.

[7] G. Crini, "Recent developments in polysaccharide-based materials used as adsorbents in wastewater treatment," *Progress in Polymer Science*, vol. 30, no. 1, pp. 38–70, 2005.

[8] R. Crisafully, M. A. L. Milhome, R. M. Cavalcante, E. R. Silveira, D. D. Keukeleire, and R. F. Nascimento, "Removal of some polycyclic aromatic hydrocarbons from petrochemical wastewater using low-cost adsorbents of natural origin," *Bioresource Technology*, vol. 99, no. 10, pp. 4515–4519, 2008.

[9] M. Rinaudo, "Chitin and chitosan: properties and applications," *Progress in Polymer Science*, vol. 31, no. 7, pp. 603–632, 2006.

[10] E. Guibal and J. Roussy, "Coagulation and flocculation of dye-containing solutions using a biopolymer (Chitosan)," *Reactive & Functional Polymers*, vol. 67, no. 1, pp. 33–42, 2007.

[11] E. Guibal, M. Van Vooren, B. A. Dempsey, and J. Roussy, "A review of the use of chitosan for the removal of particulate and dissolved contaminants," *Separation Science and Technology*, vol. 41, no. 11, pp. 2487–2514, 2006.

[12] E. Guibal, "Interactions of metal ions with chitosan-based sorbents: a review," *Separation and Purification Technology*, vol. 38, no. 1, pp. 43–74, 2004.

[13] S. Pal, Y. K. Tak, and J. M. Song, "Does the antibacterial activity of silver nanoparticles depend on the shape of the nanoparticle? A study of the gram-negative bacterium *Escherichia coli*," *Applied and Environmental Microbiology*, vol. 73, no. 6, pp. 1712–1720, 2007.

[14] B. Son, B.-Y. Yeom, S. H. Song, C.-S. Lee, and T. S. Hwang, "Antibacterial electrospun chitosan/poly(vinyl alcohol) nanofibers containing silver nitrate and titanium dioxide," *Journal of Applied Polymer Science*, vol. 111, no. 6, pp. 2892–2899, 2009.

[15] P. Danwanichakul, D. Danwanichakul, N. Sueviriyapan, and B. Sumruan, "Nylon 6/chitosan nanofibrous structures for filtration," in *Proceedings of the 1st Mae Fah Luang University International Conference*, pp. 1–8, Pathumthani, Thailand, 2012.

[16] M. T. M. Bizarria, M. A. d'Ávila, and L. H. I. Mei, "Non-woven nanofiber chitosan/PEO membranes obtained by electrospinning," *Brazilian Journal of Chemical Engineering*, vol. 31, no. 1, pp. 57–68, 2014.

[17] J. M. Deitzel, J. Kleinmeyer, D. Harris, and N. C. Beck Tan, "The effect of processing variables on the morphology of electrospun nanofibers and textiles," *Polymer*, vol. 42, no. 1, pp. 261–272, 2001.

[18] D. Rana and T. Matsuura, "Surface modifications for antifouling membranes," *Chemical Reviews*, vol. 110, no. 4, pp. 2448–2471, 2010.

[19] H. Zhang, S. Li, C. J. Branford White, X. Ning, H. Nie, and L. Zhu, "Studies on electrospun nylon-6/chitosan complex nanofiber interactions," *Electrochimica Acta*, vol. 54, no. 24, pp. 5739–5745, 2009.

[20] S. Waheed, A. Ahmad, S. M. Khan et al., "Synthesis, characterization, permeation and antibacterial properties of cellulose acetate/polyethylene glycol membranes modified with chitosan," *Desalination*, vol. 351, pp. 59–69, 2014.

[21] M. Ghani, A. A. Gharehaghaji, M. Arami, N. Takhtkuse, and B. Rezaei, "Fabrication of electrospun polyamide-6/chitosan nanofibrous membrane toward anionic dyes removal," *Journal of Nanotechnology*, vol. 2014, Article ID 278418, 12 pages, 2014.

[22] A. Sumisha, G. Arthanareeswaran, A. F. Ismail, D. P. Kumar, and M. V. Shankar, "Functionalized titanate nanotube-polyetherimide nanocomposite membrane for improved salt rejection under low pressure nanofiltration," *RSC Advances*, vol. 5, no. 49, pp. 39464–39473, 2015.

[23] N. R. Sudarshan, D. G. Hoover, and D. Knorr, "Antibacterial action of chitosan," *Food Biotechnology*, vol. 6, no. 3, pp. 257–272, 1992.

[24] S. W. Fang, C. F. Li, and D. Shih, "Antifungal activity of chitosan and its preservative effect on low-sugar candied kumquat," *Food Protect*, vol. 56, no. 2, pp. 136–140, 1994.

[25] J. K. Hwang, H. J. Kim, S. J. Yoon, and Y. R. Pyun, "Bactericidal activity of chitosan on *E.coli*," *Advances in Chitin Science*, vol. 62, no. 3, pp. 239–243, 1999.

[26] I. M. Helander, E.-L. Nurmiaho-Lassila, R. Ahvenainen, J. Rhoades, and S. Roller, "Chitosan disrupts the barrier properties of the outer membrane of Gram-negative bacteria," *International Journal of Food Microbiology*, vol. 71, no. 2-3, pp. 235–244, 2001.